532 *Inorg. Chem.* **1995,** *34,* 532–540

Articles

Synthesis, Characterization, and Electrochemical Behavior of (5,10,15-Tri-X-phenyl-2,3,7,8,12,13,17,18-octamethylcorrolato)cobalt(III) Triphenylphosphine Complexes, Where X = *p*-OCH$_3$, *p*-CH$_3$, *p*-Cl, *m*-Cl, *o*-Cl, *m*-F, *o*-F, or H

Victor A. Adamian,[†] Francis D'Souza,[†,§] Silvia Licoccia,[‡] Maria Luisa Di Vona,[‡] Emanuela Tassoni,[‡] Roberto Paolesse,[‡] Tristano Boschi,*,[‡] and Karl M. Kadish*,[†]

Department of Chemistry, University of Houston, Houston, Texas 77204-5641, and Dipartimento di Scienze e Tecnologie Chimiche, Università di Roma, Tor Vergata, 00173 Roma, Italy

Received July 22, 1994[®]

Complexes of (5,10,15-tri-X-phenyl-2,3,7,8,12,13,17,18-octamethylcorrolato)cobalt(III) triphenylphosphine, (OMTXPC)Co(PPh$_3$), where X = *p*-OCH$_3$, *p*-CH$_3$, *p*-Cl, *m*-Cl, *m*-F, *o*-Cl, *o*-F, or H, were synthesized and characterized in nonaqueous media using electrochemical, spectroelectrochemical, and EPR techniques. The *o*-Cl derivative exists as different atropisomers in solution, and a thermal interconversion between them was achieved at 338 K in toluene. Activation parameters ($\Delta S^{\ddagger}$, $\Delta H^{\ddagger}$) for interconversion between the atropisomers were obtained from ^{1}H NMR measurements and were similar in magnitude to values reported for *ortho*-substituted tetraphenylporphyrin derivatives. Formation constants for pyridine binding to the pentacoordinated cobalt(III) corroles in benzene were obtained from UV–visible spectrophotometric measurements and ranged between 20 and 193 M^{-1}, with the exact value depending upon the specific electron-donating or electron-withdrawing group on the three phenyl rings of the complex. The redox potentials of (OMTXPC)Co(PPh$_3$) also shift with the nature of the phenyl ring substituents, and linear free-energy relationships are observed. Each cobalt(III) derivative undergoes two one-electron reductions, the first of which involves a Co(III)/Co(II) conversion and concomitant loss of the bound PPh$_3$ ligand. Four one-electron oxidations are also observed for the investigated compounds, and this contrasts with the oxidative properties of related cobalt(II) porphyrins which undergo a maximum of three one-electron oxidations under similar solution conditions. The first one-electron oxidation of each cobalt(III) corrole is metal-centered and results in formation of a Co(IV) corrole as ascertained by EPR spectroscopic characterization of the electrogenerated species.

Introduction

Corroles are a class of synthetic tetrapyrrole macrocycles which have been related to both the corrins and the porphyrins.[1–4] They possess a direct bond between the two pyrrole rings (labeled as A and D in the Chart 1), and this structurally associates them with the corrins which also have such a bond but are not aromatic. At the same time, the fully-conjugated aromatic macrocycle of the corroles makes them quite close to the porphyrins which have often served as comparison compounds for describing the chemistry or physicochemical properties of the corroles.

A number of corroles and metallocorroles have been synthesized and characterized over the last 25 years,[5–18] but

Chart 1

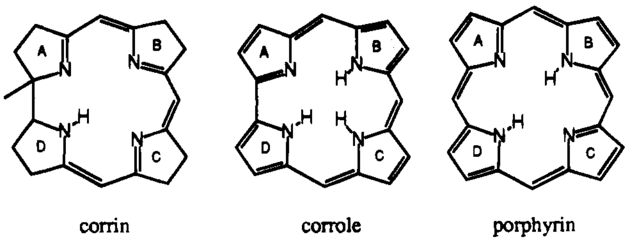

[†] University of Houston.

[‡] Università di Roma.

[§] Current address: Department of Chemistry, Wichita State University, Wichita, KS 67260-0051.

[®] Abstract published in *Advance ACS Abstracts*, December 15, 1994.

(1) Johnson, A. W. *Pure Appl. Chem.* **1970**, *23*, 375–387.

(2) Genokhova, N. S.; Melent'eva, T. A.; Berezovskii, V. M. *Russ. Chem. Rev.* **1980**, *49*, 1056–1067.

(3) Melent'eva, T. A. *Russ. Chem. Rev.* **1983**, *52*, 641–661.

(4) Licoccia, S.; Paolesse, R. *Struct. Bonding* **1994**, in press.

(5) Johnson, A. W.; Kay, I. T. *J. Chem. Soc.* **1965**, 1620–1629.

(6) (a) Conlon, M.; Johnson, A. W.; Overend, W. R.; Rajapaksa, D.; Elson, C. M. *J. Chem. Soc., Perkin Trans. I* **1973**, 2281–2288. (b) Hitchcock, P. B.; McLaughlin, G. M. *J. Chem. Soc., Dalton Trans.* **1976**, 1927–1930.

(7) Grigg, R.; Hamilton, R. J.; Jozefowicz, M. L.; Rochester C. H.; Terrel, R. J.; Wickwar, H. *J. Chem. Soc., Perkin Trans. 2*, **1973**, 407–413.

(8) Murakami, Y.; Matsuda, Y.; Yamada, S. *Chem. Lett.* **1977**, 689–692.

(9) Abeysekera, A. M.; Grigg, R.; Trocha-Grimshaw, J.; Viswanatha, V. *J. Chem. Soc., Perkin Trans. 1*, **1977**, 36–44.

(10) Murakami, Y.; Matsuda, Y.; Sakata, K.; Yamada, S.; Tanaka, Y.; Aoyama, Y. *Bull. Chem. Soc. Jpn.* **1981**, *54*, 163–169.

(11) Boschi, T.; Licoccia, S.; Paolesse, R.; Tagliatesta, P. *Inorg. Chim. Acta* **1988**, *141*, 169–171.

(12) Engel, J.; Gossauer, A.; Johnson, A. W. *J. Chem. Soc., Perkin Trans. 1*, **1978**, 871–875.

(13) Paolesse, R., Licoccia, S.; Boschi, T. *Inorg. Chim. Acta* **1990**, *178*, 9–12.

(14) Zanoni, R.; Boschi, T.; Licoccia, S.; Paolesse, R.; Tagliatesta, P. *Inorg. Chim. Acta* **1988**, *145*, 175–177.

(15) Boschi, T.; Licoccia, S.; Paolesse, R.; Tagliatesta, P.; Pelizzi, G.; Vitali, F. *J. Chem. Soc., Dalton Trans.* **1990**, 463–468.

(16) Licoccia, S.; Paci, M.; Paolesse, R.; Boschi, T. *J. Chem. Soc., Dalton Trans.* **1991**, 461–466.

(17) Paolesse, R.; Licoccia, S.; Fanciullo, M.; Morgante, E.; Boschi, T. *Inorg. Chim. Acta* **1993**, *203*, 107–114.

(18) Paolesse, R.; Licoccia, S.; Bandoli, G.; Dolmella, A.; Boschi, T. *Inorg. Chem.* **1994**, *33*, 1171–1176.

0020-1669/95/1334-0532$09.00/0

relatively little is known about the electrochemical properties of these compounds[19-24] when compared to the much studied metalloporphyrins.[25-27] Our own laboratory[24] has characterized the electrochemistry of (OMC)Co(PPh$_3$) and (OMC)Rh(PPh$_3$) in nonaqueous media and has shown that both compounds undergo three reversible one-electron oxidations within the potential limit of the solvent. This electrochemical behavior differs from that of the well-studied Co(III) and Rh(III) metalloporphyrins[25,27,28] which show only two reversible one-electron oxidations, both of which occur at the conjugated macrocycle.

The relationship between redox potentials and electron-donating or electron-withdrawing substituents has often been used to probe electronic structures as well as to shed light on the site of electron transfer in a variety of metalloporphyrins.[25,29-33] It has generally been the case that metal-centered reactions of metalloporphyrins are less sensitive to macrocyclic substituents than ring-centered ones,[25] and this observation has often been used as a diagnostic criterion to assign the site of electron transfer prior to a spectroscopic characterization of the electrooxidized or electroreduced species, either *in situ*, or as an isolated material. It is of interest to see whether the redox reactions of metallocorroles also follow linear free-energy relationships, but these types of studies could not previously be carried out since all earlier synthesized metallocorroles had the eight β-pyrrole positions occupied by alkyl groups and also had no substituents on the three *meso*-positions of the macrocycle. Recently, however, the synthesis[17,18] and structural characterization[18] of a cobalt(III) corrole which has three phenyl groups on the *meso*-positions of the macrocycle was reported, thus opening up the possibility that similar compounds with electron-donating or electron-withdrawing substituents on the three phenyl groups might be prepared in order to study the electronic effects induced by these types of substituents. Such a study should enable one not only to ascertain the influence of peripheral ring substituents on redox potentials for the corroles but should also provide data which might shed light on the cyclization reaction, a key intermediate reaction step involved in the synthesis.[17,18]

This is now examined in the present paper which reports the synthesis, pyridine binding properties, and redox potentials of eight different cobalt(III) triphenylcorrolates which contain electron-donating or electron-withdrawing substituents on the three phenyl rings of the complex. The investigated compounds are shown in Figure 1 and are represented by the formulas (OMTXPC)Co(PPh$_3$) and (OMTPC)Co(PPh$_3$), where OMTXPC is the trianion of 5,10,15-tri-X-phenyl-2,3,7,8,12,13,17,18-octamethylcorrole and X = *p*-OMe, *p*-Me, *p*-Cl, *m*-Cl, *o*-Cl, *m*-F, or *o*-F and OMTPC represents the unsubstituted derivative, *i.e.* X = H.

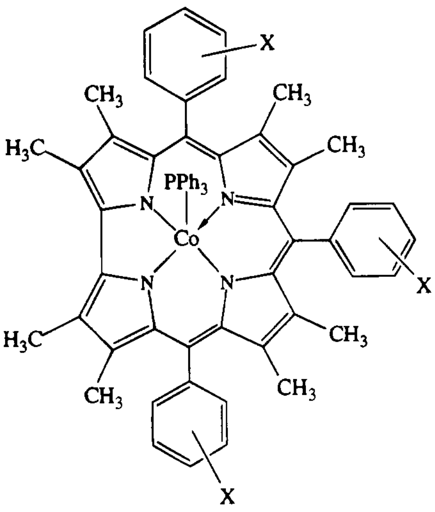

Figure 1. Structural formula of (OMTXPC)Co(PPh$_3$) complexes.

The complexes were characterized by mass spectrometry coupled with ^{1}H NMR and electronic absorption spectroscopy. All eight derivatives possess a similar structure and therefore should have a relatively constant solvation energy during each electrode process. The three phenyl groups at the *meso*-position of the unsubstituted compound are almost perpendicular to the macrocycle,[18] and this helps to hinder the aggregation that is often observed in the case of planar porphyrins and corroles. The electrochemical studies were carried out in benzonitrile, and the site of electron transfer was evaluated during each redox process using thin-layer UV–visible spectroelectrochemical and/or EPR techniques.

Experimental Section

Chemicals. Reagent grade solvents were used for synthesis of the corroles and were obtained from Carlo Erba Reagenti, Italy. Reagent grade benzonitrile (PhCN), from Aldrich Chemical Co., was vacuum-distilled over P$_2$O$_5$ prior to use. Tetra-*n*-butylammonium perchlorate, TBAP, from Eastman Kodak Co., was used as a supporting electrolyte; it was recrystallized from absolute ethanol and stored under vacuum at 40 °C.

Instrumentation. Electronic absorption spectra were recorded on a Philips PU 8700 or IBM Model 9430 spectrophotometer. Fast atom bombardment (FAB) and electronic impact (EI) mass spectra were obtained with a VG Quattro spectrometer; 3-nitrobenzyl alcohol was used as a matrix in the FAB experiment. ^{1}H NMR spectra of the cobalt corroles were recorded on a Bruker AM 400 spectrometer in C$_6$D$_6$ or C$_6$D$_5$CD$_3$. A Bruker WP80SY instrument was used to obtain ^{1}H NMR spectra of the monopyrroles used in the synthesis in CD$_3$OD. Chemical shifts are given in ppm vs tetramethylsilane (TMS).

Cyclic voltammograms were obtained with a conventional three-electrode system using an EG&G Princeton Applied Research Model 174A/175 polarographic analyzer/universal programmer. A glassy-carbon electrode was used as the working electrode, and a platinum wire, as a counter electrode. A saturated calomel electrode (SCE) was used as the reference electrode.

Spectroelectrochemical measurements were performed with a Princeton Instruments PDA-1024 diode array and ST 1000 detector controller spectrophotometer. Data acquisition and processing were

---

(19) Hush, N. S.; Dyke, J. M. *J. Inorg. Nucl. Chem.* **1973**, *35*, 4341–4347.

(20) (a) Hush, N. S.; Dyke, J. M.; Williams, M. L.; Woolsey, I. S. *J. Chem. Soc., Dalton Trans.* **1974**, 395–399. (b) Hush, N.; Woolsey, I. S. *J. Chem. Soc., Dalton. Trans.* **1974**, 24–34.

(21) Autret, M.; Will. S.; Van Caemelbecke, E.; Lex, J.; Gisselbrecht, J.-P.; Gross, M.; Vogel, E.; Kadish, K. M. *J. Am. Chem. Soc.* **1994**, *116*, 9141–9149.

(22) Matsuda, Y.; Yamada, S.; Murakami, Y. *Inorg. Chem.* **1981**, *20*, 2239–2246.

(23) Murakami, Y.; Matsuda, Y.; Yamada, S. *J. Chem. Soc., Dalton Trans.* **1981**, 855–861.

(24) Kadish, K. M.; Koh, W.; Tagliatesta, P.; Sazou, D.; Paolesse, R.; Licoccia, S.; Boschi, T. *Inorg. Chem.* **1992**, *31*, 2305–2313.

(25) Kadish, K. M. *Prog. Inorg. Chem.* **1986**, *34*, 437–605.

(26) (a) Felton, R. H. In *The Porphyrins*; Dolphyn, D., Ed.; Academic Press: New York, 1978; Vol. V, pp 53–126. (b) Davis, D. G. *Ibid.*, pp 127–152.

(27) Fuhrhop, J.-H.; Kadish, K. M.; Davis, D. G. *J. Am. Chem. Soc.* **1973**, *95*, 5140–5147.

(28) Kadish, K. M.; Han, B. C.; Endo, A. *Inorg. Chem.* **1991**, *30*, 4052–4506.

(29) Walker, F. A.; Beroiz, D.; Kadish, K. M. *J. Am. Chem. Soc.* **1976**, *98*, 3484–3489.

(30) Kadish, K. M.; Morrison, M. M. *J. Am. Chem. Soc.* **1976**, *98*, 3326–3328.

(31) Kadish, K. M.; Morrison, M. M. *Bioinorg. Chem.* **1977**, *7*, 107–115.

(32) Kadish, K. M.; Morrison, M. M. *Inorg. Chem.* **1976**, *15*, 980–982.

(33) Kadish, K. M.; Morrison, M. M.; Constant, L. A.; Dickens, L.; Davis, D. G. *J. Am. Chem. Soc.* **1976**, *98*, 8387–8390.

performed using OSMA and PSMA software. The design of the thin-layer cell for spectroelectrochemistry has been reported elsewhere.[34]

Synthesis and Characterization of Neutral Cobalt(III) Corroles. Unsubstituted (5,10,15-triphenyl-2,3,7,8,12,13,17,18-octamethylcorrolato)cobalt(III) triphenylphosphine can be prepared following four different procedures,[17,18] but the most direct approach, and the one giving the best yield, is by a direct cyclization of 3,4-dimethyl-2-(α-hydroxybenzyl)pyrrole.[18] We have now extended this one-step synthetic procedure to pyrroles bearing different substituents on the 2-phenyl ring and have succeeded in the synthesis of seven new cobalt(III) corroles. The (5,10,15-tri-X-phenyl-2,3,7,8,12,13,17,18-octamethylcorrolato)cobalt(III) triphenylphosphine complexes, where X = *p*-OMe, *p*-Me, *p*-Cl, *m*-Cl, *o*-Cl, *m*-F, or *o*-F were prepared by direct cyclization of 3,4-dimethyl-2-(α-hydroxyl-X-benzyl)pyrroles-5-carboxylic acids.[18] The substituted 3,4-dimethyl-2-(α-hydroxyl-X-benzyl)pyrroles-5-carboxylic acids were prepared by following a procedure published for the unsubstituted pyrrole, i.e., 3,4-dimethyl-2-(α-hydroxybenzyl)pyrrole-5-carboxylic acid.[17] The ^{1}H NMR and mass spectral data of these pyrroles are given below.

3,4-Dimethyl-2-(α-hydroxyl-*p*-OMe-benzyl)pyrrole-5-carboxylic acid. ^{1}H NMR (δ): 6.95−7.60 (*d.d.*, 4 H, −Ph); 5.60 (*s*, 1 H, 2-CH); 3.80 (*s*, 3 H, *p*-OMe); 2.20 (*s*, 3 H, 3-Me); 1.90 (*s*, 3H, 4-Me). MS [*m/z* (%)]: 273 (20%) [$M^+ - 1$]. Yield: 49%.

3,4-Dimethyl-2-(α-hydroxyl-*p*-Me-benzyl)pyrrole-5-carboxylic acid. ^{1}H NMR (δ): 7.10 (*m*, 4 H, -Ph); 5.80 (*s*, 1 H, 2-CH); 2.30 (*s*, 3 H, *p*-Me); 2.20 (s, 3 H, 3-Me); 1.82 (s, 3H, 4-Me). MS [*m/z* (%)]: 258.6 (63%) [M^+]. Yield: 68%.

3,4-Dimethyl-2-(α-hydroxyl-*p*-Cl-benzyl)pyrrole-5-carboxylic acid. ^{1}H NMR (δ): 7.34 (*m*, 4 H, −Ph); 5.86 (*s*, 1 H, 2-CH); 2.26 (*s*, 3 H, 3-Me); 1.90 (*s*, 3H, 4-Me). MS [*m/z* (%)]: 278.7 (2%) [M^+]. Yield: 85%.

3,4-Dimethyl-2-(α-hydroxyl-*m*-Cl-benzyl)pyrrole-5-carboxylic acid. ^{1}H NMR (δ): 7.4−7.28 (*m*, 4 H, Ph); 5.86 (*s*, 1 H, 2-CH); 2.24 (*s*, 3 H, 3-Me); 1.90 (*s*, 3 H, 4-Me). MS [*m/z* (%)]: 278.7 (30%) [M^+], 280.5 (10%) [$M^+ + 2$] (isotopic cluster chlorine atom). Yield: 88%.

3,4-Dimethyl-2-(α-hydroxyl-*o*-Cl-benzyl)pyrrole-5-carboxylic acid. ^{1}H NMR (δ): 7.45 (*m*, 4 H, −Ph); 6.15 (*s*, 1 H, 2-CH); 2.20 (s, 3 H, 3-Me); 1.86 (*s*, 3H, 4-Me). MS [*m/z* (%)]: 277 (8%) [M^+], 279 (2.5%) [$M^+ + 2$] (isotopic cluster chlorine atom). Yield: 79%.

3,4-Dimethyl-2-(α-hydroxyl-*m*-F-benzyl)pyrrole-5-carboxylic acid. ^{1}H NMR (δ): 7.20 (*m*, 4 H, -Ph); 5.85 (*s*, 1 H, 2-CH); 2.25 (*s*, 3 H, 3-Me); 1.90 (*s*, 3H, 4-Me). MS [*m/z* (%)]: 262.8 (34%) [$M^+ - 1$]. Yield: 60%.

3,4-Dimethyl-2-(α-hydroxyl-*o*-F-benzyl)pyrrole-5-carboxylic acid. ^{1}H NMR (δ): 7.20 (*m*, 4 H, −Ph); 6.12 (*s*, 1 H, 2-CH); 2.26 (*s*, 3 H, 3-Me); 1.86 (s, 3H, 4-Me). MS [*m/z* (%)]: 262 (12%) [$M^+ - 1$]. Yield: 56%.

Synthesis of (OMTXPC)Co(PPh$_3$). In a typical experiment the starting pyrrole (2.0 mmol) was dissolved in hot absolute ethanol (200 mL); trifluoroacetic acid (1 mL) was then added and the solution refluxed for 15 min. Excesses of sodium acetate (20.0 mmol), cobalt(II) acetate (1.9 mmol), and triphenylphosphine (2.0 mmol) were then added, and the solution was refluxed for 24 h. The solvent was vacuum evaporated and the residue extracted with diethyl ether. Column chromatography on basic alumina (Merck, type T) using diethyl ether as eluant, followed by recrystallization from 1:3 CH_2Cl_2/MeOH afforded pure products. (OMC)Co(PPh$_3$) was prepared according to the published procedure.[24] Spectral properties and analytical data for the (OMTXPC)Co(PPh$_3$) complexes are given below.

(OMT*p*-OMePC)Co(PPh$_3$). ^{1}H NMR (δ): 7.81−7.00 (*m*, 12H, phenyl-H); 6.85 (*br*, 3H, *p*-PPh$_3$); 6.67 (*br*, 6H, *m*-PPh$_3$); 5.41 (*br*, 6H, *o*-PPh$_3$); 3.57 (*s*, 3H, 10-*p*-OMe); 3.56 (*s*, 6H, 5,15-*p*-OMe); 3.17 (*s*, 6H, 2,18-Me); 2.47 (*s*, 6H, 3,17-Me); 2.46 (*s*, 6H, 7,13(or 8,12)-Me); 2.45 (*s*, 6H, 8,12(or 7,13)-Me). MS (*m/z*): 1047 [M^+]. λ_{max} (ε): 382 (46 500), 572 nm (8200). Yield: 20%. Anal. Calcd for $C_{66}H_{60}N_4O_3PCo$: C, 75.70; H, 5.78; N, 5.35. Found: C, 75.40; H, 5.90; N, 5.05.

(OMT*p*-MePC)Co(PPh$_3$). ^{1}H NMR (δ): 7.87−7.07 (*m*, 12H, phenyl-H); 6.86 (*t*, *J* = 7 Hz, 3H, *p*-PPh$_3$); 6.78 (*t*, *J* = 7 Hz, 6H, *m*-PPh$_3$); 5.41 (*t*, *J* = 7 Hz, 6H, *o*-PPh$_3$); 3.15 (*s*, 6H, 2,18-Me); 2.45 (*s*, 6H, 3,17-Me); 2.43 (*s*, 15 H, 7,13(or 8,12)-Me + 5,10,15-*p*-Me); 2.39 (*s*, 6H, 8,12(or 7,13)-Me). MS (*m/z*): 999 [M^+]. λ_{max} (ε): 379 (55 000), 414 sh (34 600), 572 nm (9 200). Yield: 20%. Anal. Calcd for $C_{66}H_{60}N_4PCo$: C, 79.34; H, 6.05; N, 5.61. Found: C, 79.60; H, 6.15; N, 5.50.

(OMT*p*-ClPC)Co(PPh$_3$). ^{1}H NMR (see Figure 3) (δ): 7.58−7.01 (*m*, 12H, phenyl-H); 6.81 (*t*, *J* = 7 Hz, 3H, *p*-PPh$_3$); 6.59 (*t*, *J* = 7 Hz, 6H, *m*-PPh$_3$); 5.22 (*t*, *J* = 7 Hz, 6H, *o*-PPh$_3$); 3.12 (*s*, 6H, 2,18-Me); 2.31 (*s*, 6H, 3,17-Me); 2.26 (*s*, 6 H, 7,13(or 8,12)-Me); 2.23 (*s*, 6H, 8,12(or 7,13)-Me). MS (*m/z*): 1059 [M^+], 1061 [$M^+ + 2$], 1063 [$M^+ + 4$], 1065 [$M^+ + 6$] (isotopic cluster of three chlorine atoms). λ_{max} (ε): 380 (21 700), 412 sh (14 600), 574 nm (3300). Yield: 10%. Anal. Calcd for $C_{63}H_{51}N_4Cl_3PCo$: C, 71.36; H, 4.85; N, 5.28. Found: C, 71.00; H, 4.65; N, 5.10.

(OMT*m*-ClPC)Co(PPh$_3$). ^{1}H NMR (see Figure 3) (δ): 7.93−6.86 (*m*, 12H, phenyl-H); 6.86 (*t*, *J* = 7 Hz, 3H, *p*-PPh$_3$); 6.59 (*t*, *J* = 7 Hz, 6H, *m*-PPh$_3$); 5.20 (*br*, 6H, *o*-PPh$_3$); 3.22−3.09 (*br*, 6H, 2,18-Me); 2.37−2.27 (18H, 3,7,8,12,13,17-Me). MS (*m/z*): 1059 [M^+], 1061 [$M^+ + 2$], 1063 [$M^+ + 4$], 1065 [$M^+ + 6$] (isotopic cluster of three chlorine atoms). λ_{max} (ε): 380 (51 700), 411 sh (38 500), 576 nm (8800). Yield: 8%. Anal. Calcd for $C_{63}H_{51}N_4Cl_3PCo$: C, 71.36; H, 4.85; N, 5.28. Found: C, 71.10; H, 4.70; N, 5.15.

(OMT*o*-ClPC)Co(PPh$_3$). ^{1}H NMR (see Figure 3) (δ): 7.87−7.06 (*m*, 12H, phenyl-H); 6.83 (*m*, 3H, *p*-PPh$_3$); 6.63 (*m*, 6H, *m*-PPh$_3$); 5.44 (*t*, *J* = 7 Hz, 6H, *o*-PPh$_3$); 3.08, 3.02, 2.95 (*s*, 6H, 2,18-Me); 2.56−2.42 (18H, 3,7,8,12,13,17-Me). MS (*m/z*): 1059 [M^+], 1061 [$M^+ + 2$], 1063 [$M^+ + 4$], 1065 [$M^+ + 6$] (isotopic cluster of three chlorine atoms). λ_{max} (ε): 378 (50 500), 414.5 sh (35 700), 578 nm (8100). Yield: 10%. Anal. Calcd for $C_{63}H_{51}N_4Cl_3PCo$: C, 71.36; H, 4.85; N, 5.28. Found: C, 71.55; H, 4.95; N, 5.10.

(OMT*m*-FPC)Co(PPh$_3$). ^{1}H NMR (δ): 7.59−7.18 (*br*, 12H, phenyl-H); 6.81 (*t*, *J* = 7 Hz, 3H, *p*-PPh$_3$); 6.58 (*br*, 6H, *m*-PPh$_3$); 5.19 (*br*, 6H, *o*-PPh$_3$); 3.14 (*s*, 6H, 2,18-Me); 2.36 (*s*, 6H, 3,17-Me); 2.34 (*s*, 6H, 7,13(or 8,12)-Me); 2.29 (*s*, 6H, 8,12(or 7,13)-Me). MS (*m/z*): 1011 [M^+]. λ_{max} (ε): 378 (54 000), 411 (38 600), 576 nm (8900). Yield: 5%. Anal. Calcd for $C_{63}H_{51}N_4F_3PCo$: C, 74.84; H, 5.08; N, 5.54. Found: C, 75.15; H, 5.20; N, 5.65.

(OMT*o*-FPC)Co(PPh$_3$). ^{1}H NMR (δ): 7.70−7.04 (*br*, 12H, phenyl-H); 6.85 (*br*, 3H, *p*-PPh$_3$); 6.69 (*br*, 6H, *m*-PPh$_3$); 5.38 (*br*, 6H, *o*-PPh$_3$); 3.14−3.00 (*s*, 6H, 2,18-Me); 2.61−2.32 (*s*, 18H, 3,7,8,12,13,17-Me). MS (*m/z*): 1011 [M^+]. λ_{max} (ε): 379 (57 000), 410 (42 500), 578 nm (10 400). Yield: 10%. Anal. Calcd for $C_{63}H_{51}N_4F_3PCo$: C, 74.84; H, 5.08; N, 5.54. Found: C, 75.00; H, 5.15; N, 5.60.

Equilibrium Measurements. The binding of pyridine to the Co(III) corroles was carried out at 25 °C in benzene (Aldrich 99+%) and the reaction monitored by UV−visible spectroscopy. The concentration of the corrole for these measurements was $\sim 10^{-5}$ M, and that of pyridine was in the range of 10^{-3} to 0.5 M. The absorbance data were corrected for dilution and then fitted to the following equation by means of a nonlinear least-squares procedure

$$A = \frac{A_0 + A_\infty K[\mathrm{Py}]}{1 + K[\mathrm{Py}]} \tag{1}$$

where *A* is the absorbance measured at a given pyridine concentration, A_0 is the absorbance of the substrate at [Py] = 0, and A_∞ refers to the absorbance of the substrate when fully coordinated by pyridine. The quantities A_∞ and *K* were treated as adjustable parameters.

Results and Discussion

Synthesis. The synthesis of porphyrins and chlorins from monopyrroles has long been known[35] but the preparation of a corrole such as (OMTPC)Co(PPh$_3$) from a monopyrrolic precursor has only recently been reported in the literature.[18] Key factors driving the reaction toward formation of a contracted corrole ring are the peculiar catalytic activity of the cobalt atom in the presence of PPh$_3$ and the steric release allowed by the corrole moiety. In fact, despite the steric hindrance of the

---

(34) Lin, X. Q.; Kadish, K. M. *Anal. Chem.* **1985**, *57*, 1498−1501.

(35) Kim, J. B.; Adler, A. D.; Longo, F. R. In *The Porphyrins*; Dolphin, D., Ed.; Academic Press: New York, **1978**; Vol. IA, pp 85−100.

β-pyrrole and *meso*-phenyl substituents, the corrole can mantain a planar conformation.[18] This differs from the related porphyrins where peripheral crowding causes severe deviations from planarity. The extension of our published synthetic procedure to corroles bearing different substituents on the 2-phenyl ring leads to compounds where steric release is still present. This is true, even in the case of the compounds with a bulky *o*-Cl substituent, as demonstrated by the spectral properties of the (OMT*o*-ClPC)Co(PPh_3) complex. Aromaticity, and hence planarity, is in fact demonstrated both by the presence of intense absorptions due to transitions within the π system of the macrocycle and by the strong upfield shift of all ^1H NMR resonances of the neutral compound due to the macrocycle ring current.

The best yields of (OMTXPC)Co(PPh_3) were as high as 20% and were obtained for the complexes with electron-donating substituents (*p*-OMe or *p*-Me) on the phenyl rings. Lower yields (5−10%) were obtained for the halide-substituted compounds (X = Cl or F). Attempts were also made to synthesize the NO_2 derivatives, but no cyclization reaction was observed for phenyl rings bearing this strong electron-withdrawing group. These results are in agreement with a mechanism formulated for the acid-catalyzed cyclization reaction of 2-α-hydroxypyrroles involving cationic species generated by elimination of water from the protonated form of the starting pyrrole.[35] These cationic species should, in fact, be stabilized by the presence of electron-donating substituents. Porphyrins are the products of cyclization when metal ions different from cobalt are used.[18] It can be assumed that the mechanisms leading to porphyrin or corrole syntheses differs only after the formation of a tetrapyrrole.[18]

Axial Binding of Pyridine. The spectral changes seen upon addition of the pyridine to the (OMTXPC)Co(PPh_3) complexes are consistent with addition of a single pyridine molecule and establishment of the following equilibrium:

$$\text{(OMTXPC)Co(PPh}_3\text{)} + \text{Py} \leftrightharpoons \text{(OMTXPC)Co(PPh}_3\text{)(Py)} \tag{2a}$$

$$K = \frac{[\text{(OMTXPC)Co(PPh}_3\text{)(Py)}]}{[\text{(OMTXPC)Co(PPh}_3\text{)}][\text{Py}]} \tag{2b}$$

The resulting hexacoordinated corrole has a UV-vis spectrum which is significantly different from that of the pentacoordinated one, with the most peculiar feature being a large (ca. 60 nm) bathochromic shift of the absorption maximum. An example of the observed spectral changes during the titration are shown in Figure 2a for the case of (OMT*p*-OMePC)Co(PPh_3).

A summary of the calculated formation constants is given in Table 1. The values range from 20 to 35 M^{-1} for the OMTXPC derivatives and are 1 order of magnitude smaller than for the formation of (OMC)Co(PPh_3)(py) from (OMC)Co(PPh_3). The decrease of the equilibrium constant upon going from (OMC)Co(PPh_3) to (OMTPC)Co(PPh_3), *i.e.*, upon substituting the *meso*-hydrogens with phenyl groups, can be attributed to the influence of the steric factors. The values of the equilibrium constant are, however, comparable to values previously reported for the binding of substituted pyridines to cobalt *β*-alkylcorroles.[36]

A change in the phenyl ring substituents over the series of compounds results in only a small change in the magnitude of equilibrium constant. However, the *K* values show a good correlation with the Hammett substituent constant, 3σ (Figure 2b). As expected, the pyridine binding reaction is favored by electron-withdrawing substituents ($\varrho = 0.58$).

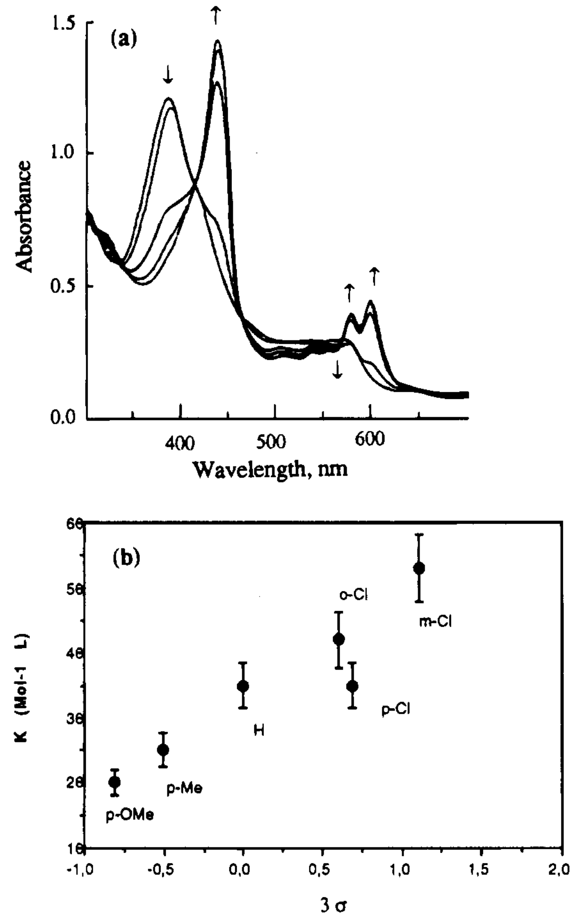

Figure 2. (a) Changes in electronic absorption spectra of (OMT*p*-OMePC)Co(PPh_3) in benzene upon addition of pyridine and (b) substituent effects on equilibrium constants for the binding of pyridine to (OMTXPC)Co(PPh_3). Error bars correspond to 10% of *K* values.

Table 1. Equilibrium Constants for Formation of (OMTXPC)Co(PPh_3)(py) from (OMTXPC)Co(PPh_3) in Benzene at 25 °C

corrole ligand	*K* (M^{-1})	corrole ligand	*K* (M^{-1})
OMT*p*-OMePC	20(±2)	OMT*m*-ClPC	53 (±2)
OMT*p*-MePC	25(±3)	OMT*o*-ClPC	42 (±4)
OMTPC	35(±2)	OMC	193(±11)
OMT*p*-ClPC	35(±3)		

NMR Studies. Assignment of proton resonances on (OMTXPC)Co(PPh_3) was made on the basis of symmetry considerations, on shielding effects of the *meso*-phenyl groups, and by comparison with previously-reported NMR data for (OMTPC)Co(PPh_3).[17,18] A summary of ^1H NMR data for these compounds is given in the Experimental Section, and spectra for the *o*-, *m*-, and *p*-chloro-substituted derivatives are shown in Figure 3. An increase in the line widths is observed upon going from the *p*-Cl derivative (trace a) to the *m*-Cl one (trace b). These resonances are split into three major components, which, in the case of the *o*-Cl complex, are labeled as A, B, and C, as shown in Figure 4.

The multitude of resonances for the *o*-Cl-substituted corrole can be explained by the presence of stable atropisomers at room temperature (*i.e.*, geometric isomers which are stable by virtue of restricted rotation about a formal single bond) as a result of the chlorine atoms located on either side of the macrocyclic ring. In fact, the presence of the bound PPh_3 axial ligand makes the two faces of the complex diastereotopic. Numerous

---

(36) Murakami, Y.; Yamada, S.; Matsuda, Y.; Sakata, K. *Bull. Chem. Soc. Jpn.* **1978**, *51*, 123−129.

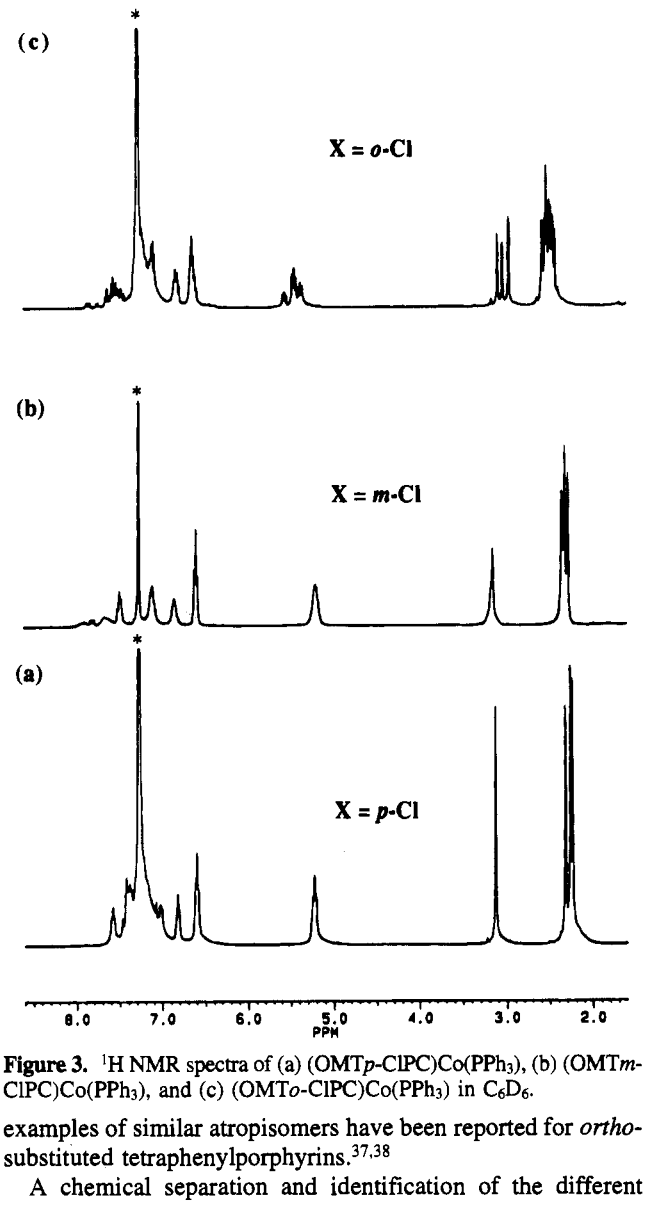

Figure 3. ^{1}H NMR spectra of (a) (OMT*p*-ClPC)Co(PPh$_3$), (b) (OMT*m*-ClPC)Co(PPh$_3$), and (c) (OMT*o*-ClPC)Co(PPh$_3$) in C_6D_6.

examples of similar atropisomers have been reported for *ortho*-substituted tetraphenylporphyrins.[37,38]

A chemical separation and identification of the different corrole atropisomers is beyond the scope of the present work. However, thermal interconversion was achieved at 338 K in toluene. The formation of an equilibrium mixture is best evidenced by a coalescence of resonances due to the *ortho* protons on the phenyl rings of PPh$_3$ as shown in Figure 4.

Activation parameters for interconversion of the atropisomers from the isomerization rate constants of peaks A, B, and C in Figure 4 were obtained by using Eyring's equation.[39] The values thus obtained are summarized in Table 2. The free energy barrier is similar for the three investigated components and is comparable to values obtained for other similar compounds having different atropisomers.[39] This is true despite the fact that the interconversion rate constants are different for resonances B and C with respect to resonance A in Figure 4, thus indicating a different local flexibility in the side chain motion. However, the measured activation enthalpies and entropies are very similar for all three resonances which suggests that no single atropisomer is favored at room temperature.

Electroreduction. Figure 5a shows a cyclic voltammogram for the oxidation and reduction of (OMT*p*-ClPC)Co(PPh$_3$) in PhCN, 0.2 M TBAP. The compound undergoes two one-electron reductions, the first (process I) of which is irreversible with E_{pc} located at −0.89 V vs SCE for a scan rate of 0.1 V/s. Reversing the scan after the first reduction results in a reoxidation peak (process I′) located at $E_{pa} = -0.31$ V. The second reduction, process II, is located at $E_{1/2} = -1.90$ V, a value close to the potential limit of the solvent. Similar electroreduction behavior is observed for each investigated corrole, and the corresponding half-wave or peak potentials are summarized in Table 3.

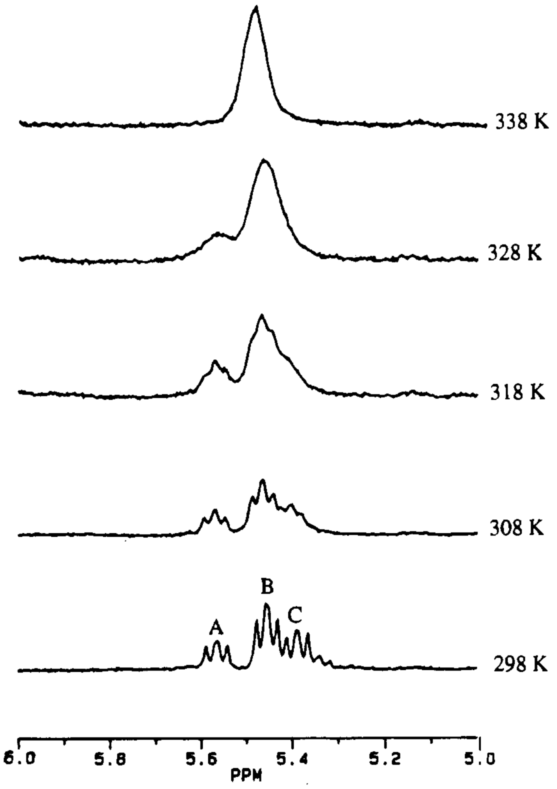

Figure 4. Temperature dependence of *o*-proton resonances for the axial PPh$_3$ ligand of (OMT*o*-ClPC)Co(PPh$_3$) in $C_6D_5CD_3$.

Table 2. Rate Constants and Activation Parameters for Thermal Interconversion of the Co(OMT*o*-ClPC)(PPh$_3$) Atropisomers, with Labels of the Resonances Shown in Figure 4

resonance	k (s^{-1})	$\Delta G^{\ddagger}$ (kcal/mol)	$\Delta H^{\ddagger}$ (kcal/mol)	$\Delta S^{\ddagger}$ (eu)
A	1.9×10^{-2}	17.3	16.3	−3.0
B	2.0×10^{-2}	17.2	15.6	−5.6
C	7.5×10^{-3}	16.7	15.2	−5.0

A comparison between the redox behavior of (OMT*p*-ClPC)-Co^{III}(PPh$_3$) and a mono-PPh$_3$-bound porphyrin analog, (T*p*-ClPP)Co^{II}(PPh$_3$), where T*p*-ClPP is the dianion of the *meso*-tetra-*p*-Cl-phenylporphyrin, is shown in Figure 5b. The porphyrin complex, (T*p*-ClPP)Co^{II}(PPh$_3$), was prepared by addition of 1.0 equiv PPh$_3$ to (T*p*-ClPP)Co in PhCN.[40] The resulting five-coordinate complex undergoes two reversible one-electron reductions (processes I and II) which are located at $E_{1/2} = -0.82$ and −1.91 V. These values can be compared to an $E_{pc} = -0.89$ V and an $E_{1/2} = -1.90$ V for the two one-electron reductions of (OMT*p*-ClPC)Co(PPh$_3$). Also, as shown in Figure 5, peak potentials for reduction of the cobalt corrole and cobalt porphyrin are almost identical upon the cathodic scan. This

---

(37) Walker, F. A. *Tetrahedron Lett.* **1971**, 4949–4951.

(38) Freitag, R. A.; Mercer-Smith, J. A.; Whitten, D. G. *J. Am. Chem. Soc.* **1981**, *103*, 1226–1228.

(39) Testa, B. *Principles of Organic Stereochemistry*; Marcel Dekker: New York, 1979.

(40) (a) Wayland, B. B.; Abd-Elmageed, M. E. *J. Am. Chem. Soc.* **1974**, *96*, 4809–4814. (b) Wayland, B. B.; Sherry, A. E.; Bunn, A. G. *J. Am. Chem. Soc.* **1993**, *115*, 7675–7684.

(41) Safo, M. K.; Walker, F. A.; Raitsimring, A. M.; Walters, W. P.; Dolata, D. P.; Debrunner, P. G.; Scheidt, W. R. *J. Am. Chem. Soc.* **1994**, *116*, 7760–7770.

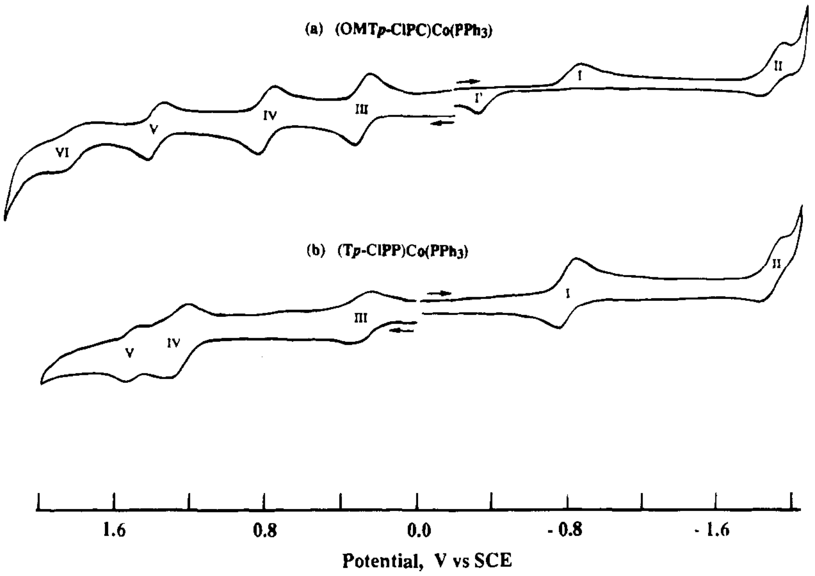

Figure 5. Cyclic voltammograms of (a) (OMT*p*-ClPC)Co(PPh_3) and (b) (T*p*-ClPP)Co(PPh_3) in PhCN, 0.2 M TBAP. Scan rate = 0.1 V/s.

Table 3. Half-Wave Potentials (V vs SCE) for the Oxidation and Reduction of (OMT*p*-XPC)Co(PPh_3) in PhCN, 0.2 M TBAP

					reduction		
		oxidation			1st		
substituent[a]	3σ	3rd	2nd	1st	E_{pc}	E_{pa}	2nd
p-OMe	−0.81	1.39[b]	0.76	0.22	−1.0	−0.38	−1.96
p-Me	−0.51	1.41	0.78	0.23	−1.01	−0.38	−1.97
H	0.0	1.43	0.80	0.24	−1.00	−0.34	−1.96
o-Cl	0.60	1.51	0.88	0.33	−0.80	−0.32	−1.88
p-Cl	0.69	1.45	0.85	0.31	−0.89	−0.31	−1.90
o-F	0.72	1.57	0.89	0.31	−0.86	−0.30	−1.93
m-F	1.02	1.51	0.86	0.32	0.84	−0.32	−1.92
m-Cl	1.11	1.53	0.88	0.30	−0.92	−0.32	−1.93
(OMC)Co(PPh_3)[c]		1.54	0.76	0.19	−0.86	−0.30	−1.92

[a] See Figure 1. [b] Irreversible process. Value given is E_{pa} at a scan rate = 0.1 V/s. [c] Potentials taken from ref 24.

close similarity in potentials might suggest that the initial oxidation state of the metal is the same for the two macrocyclic complexes or, alternatively, that the electron density distribution in the trianionic corrole macrocycle containing a cobalt(III) ion is the same as in the dianionic porphyrin containing a cobalt(II) ion. The first possibility seems unlikely, but in order to further investigate this point, we spectroscopically examined the species formed after the first one-electron reduction of both compounds. These results are discussed below.

The neutral cobalt(III) corroles are all characterized by a Soret band at 380−390 nm, a shoulder at 410−420 nm, and a broad visible absorption band centered at around 580 nm. Controlled potential reduction of (OMTPC)Co(PPh_3) at −1.3 V in a thin-layer spectroelectrochemical cell leads to a disappearance of the original Soret band at 380 nm and the appearance of a new red-shifted Soret band located at around 430 nm (see Figure 6a). The spectral changes are reversible, and reoxidation of the singly-reduced species at a controlled potential of 0.0 V leads to complete recovery of the initial UV−vis spectrum. A similar behavior has been reported for (OMC)Co(PPh_3)[24] and, when combined with the noncoupled reduction and reoxidation peaks for the first reduction of (OMT*p*-ClPC)Co(PPh_3) (Figure 5), suggests a metal-centered reduction, *i.e.*, a Co(III)/Co(II) reaction followed by a coupled chemical reaction.

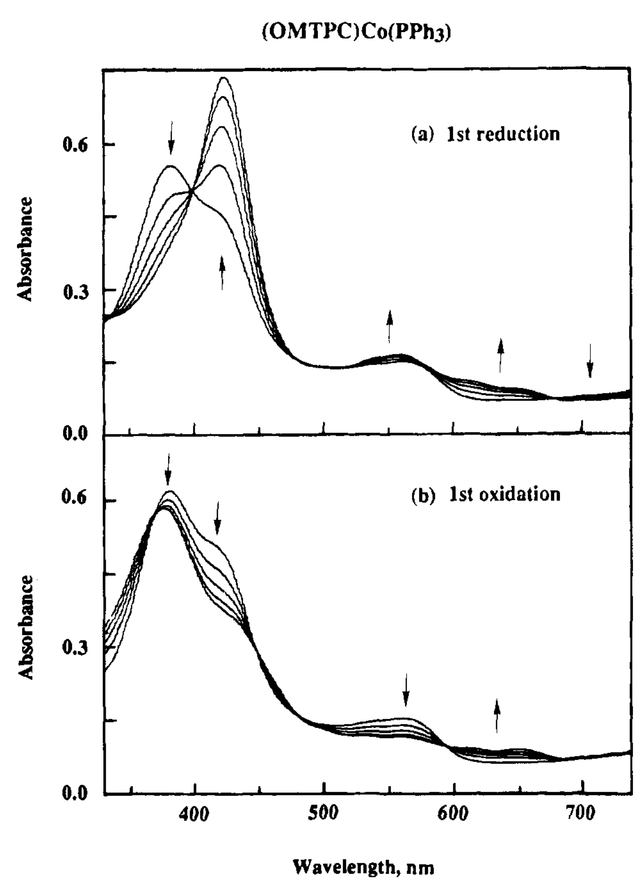

Figure 6. Thin-layer spectral changes obtained for (OMTPC)Co(PPh_3) in PhCN, 0.1 M TBAP during (a) the first reduction and (b) the first oxidation.

The noncoupled peaks for the first reduction of the Co(III) corroles can be interpreted by invoking a loss of the triphenylphosphine axial ligand after generation of Co(II) and a change from square pyramidal to planar geometry for the compound, which is then reoxidized at a more positive potential. The EPR spectrum obtained after bulk electroreduction of (OMTPC)Co^{III}(PPh_3) at −1.3 V in PhCN under nitrogen at 77 K is shown in Figure 7a and also supports this mechanism. The rhombic signal shows three principal *g* values with partially resolved hyperfine splitting due to the ^{59}Co nuclear interaction. There is no additional hyperfine splitting due to the phosphorous nucleus of PPh_3, in agreement with axial ligand dissociation after the first one-electron reduction. Three major components of the Co(II) spectrum are located at $g_1 = 3.349$, $g_2 = 2.187$,

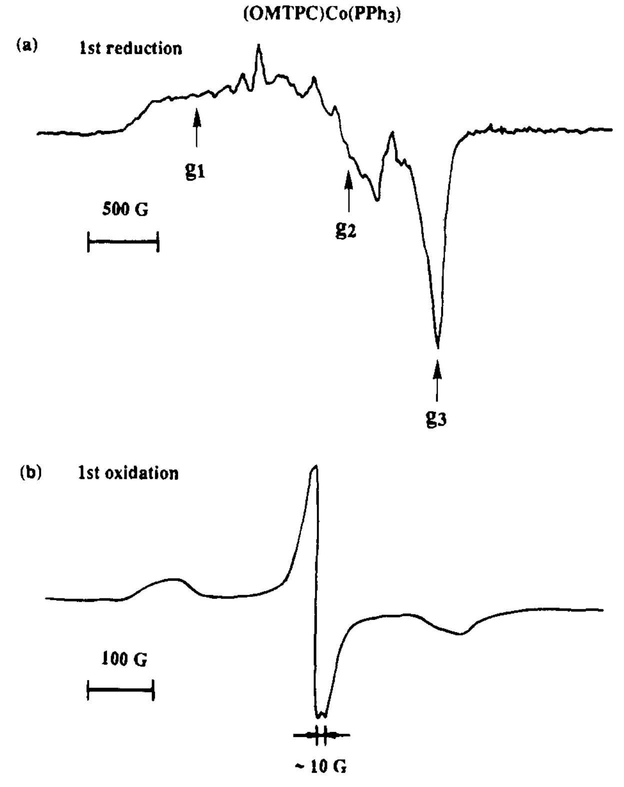

Figure 7. EPR signals obtained for (OMTPC)Co(PPh$_3$) after (a) the first reduction and (b) the first oxidation in PhCN, 0.2 M TBAP.

and $g_3 = 1.903$. The hyperfine coupling originating from the ^{59}Co ($I = {}^7/_2$) nucleus is resolved only in the low-field part of the spectrum, and the calculated values are at $A_1{}^{Co} = 181 \times 10^{-4}$ cm^{-1} and $A_2{}^{Co} = 76 \times 10^{-4}$ cm^{-1}. The g and A values both agree with literature results for other cobalt(II) corroles.[10,21]

The UV–visible changes observed during controlled potential electroreduction of (T*p*-ClPP)Co(PPh$_3$) in a thin-layer cell are shown in Figure 8a. The electroreduction is accompanied by a decrease in intensity of the 410 nm Soret band and the formation of a new split Soret band located at 360 and 420 nm. The final spectrum has been well characterized in the literature and assigned to that of a Co(I) metalloporphyrin.[42–44] These results thus clearly confirm that the initial oxidation state of the central metal ion, when bound to a PPh$_3$ axial ligand, is +3 in the case of the cobalt corroles as opposed to +2 in the case of cobalt porphyrins.

Electrooxidation. (OMT*p*-ClPC)Co(PPh$_3$) undergoes four one-electron oxidations which are labeled as processes III–VI in Figure 5a. The first three are reversible, while the fourth is quasireversible and close to the anodic potential limit of the solvent. This behavior contrasts with that of (T*p*-ClPP)Co^{II}(PPh$_3$), which undergoes only three one-electron oxidations (processes III–V), the first of which involves a Co(II)/Co(III) transition (see Figure 5b). The potential separation, $\Delta E_{1/2}$, between processes III and IV of (T*p*-ClPP)Co(PPh$_3$) is 0.96 V, while $\Delta E_{1/2}$ between processes IV and V of the same compound is 0.29 V, a value close to the $\Delta E_{1/2}$ for the successive one-electron ring-centered oxidations of most metalloporphyrins.[25] The absolute potential difference in $E_{1/2}$ between any two successive oxidations of (OMT*p*-ClPC)Co(PPh$_3$) varies between 0.55 and 0.65 V, and similar results are obtained for the other seven investigated cobalt(III) corroles (see Table 3).

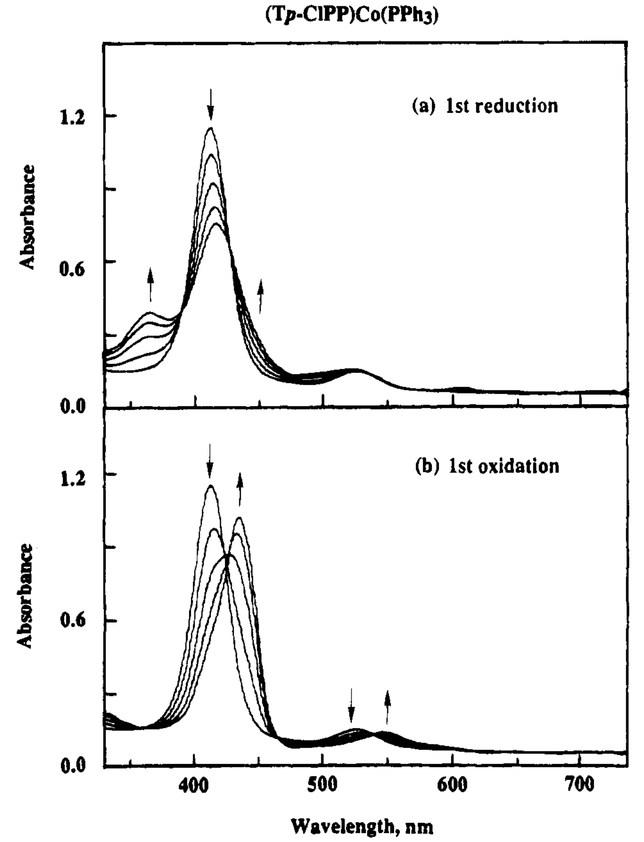

Figure 8. Thin-layer spectral changes obtained for (T*p*-ClPP)Co(PPh$_3$) in PhCN, 0.1 M TBAP during (a) the first reduction and (b) the first oxidation.

The abstraction of one electron from (OMTXPC)Co(PPh$_3$) can involve the conjugated macrocycle with formation of a cobalt(III) corrole π-cation radical or it may involve the metal with formation of a cobalt(IV) derivative. As seen in Figure 6b, the first oxidation of (OMTPC)Co(PPh$_3$) leads to a decrease of the Soret band intensity at ~380 nm and to an almost complete disappearance of the visible band at 560 nm. The first one-electron oxidation of (T*p*-ClPP)Co^{II}(PPh$_3$) also leads to a decrease in intensity of the Soret and visible bands which are located at 410 and 525 nm, and this is accompanied by the concomitant appearance of new red-shifted Soret and visible bands at 435 and 545 nm (see Figure 8b). The spectral changes observed upon the first one-electron oxidation are typical for a metal-centered process in the case of metalloporphyrins,[43,44] where a Co(II)/Co(III) reaction is observed, but do not allow us to make a firm conclusion as to the site of electron transfer upon oxidation of the cobalt(III) corroles. However, as discussed below, the EPR spectra of the species obtained after the first one-electron oxidation of (OMTPC)Co(PPh$_3$) suggest a metal-centered oxidation and formation of a Co(IV) derivative.

The EPR spectra obtained after the first one-electron oxidation of (OMTPC)Co(PPh$_3$), (OMT*m*-FPC)Co(PPh$_3$), and (OMT*m*-ClPC)Co(PPh$_3$) in PhCN are similar to each other and reveal spectral features different from those of cobalt(III) porphyrin π-cation radicals reported in the literature.[44,45] The signals of the singly-oxidized corrole species have a central line at $g = 2.002$ which is similar to values reported for cobalt(III) porphyrin π-cation radicals.[45] However, the shape of the overall signal in Figure 7b differs from that of most porphyrin π-cation radicals in that two additional broad peaks with a separation of

---

(42) Felton, R. H.; Linschitz, H. *J. Am. Chem. Soc.* **1966**, *88*, 1113–1116.

(43) D'Souza, F.; Villard, A.; Van Caemelbecke, E.; Franzen, M.; Boschi, T.; Tagliatesta, P.; Kadish, K. M. *Inorg. Chem.* **1993**, *32*, 4042–4048.

(44) Kadish, K. M.; Lin, Q. X.; Han, B. C. *Inorg. Chem.* **1987**, *26*, 4161–4167.

(45) (a) Wolberg, A., Manassen, J. *J. Am. Chem. Soc.* **1970**, *92*, 2982–2991. (b) Ichimori, K.; Ohya-Nishiguchi, H.; Hirota, N.; Yamamoto, K. *Bull. Chem. Soc. Jpn.* **1985**, *58*, 623–630.

about 400 G are also seen on either side of the central line. Increasing the temperature results in a lowering of intensity for these two broad peaks, but a complete isotropic radical signal could not be obtained. This EPR spectrum cannot be assigned to a triplet magnetic spin state which might result upon formation of a $\pi-\pi$ dimer of the corrole π-cation radical since neither the expected two additional satellite peaks of lower intensity nor the half-field signal[46] is observed.

The EPR spectrum in Figure 7b can thus be assigned to either a pure π-cation radical of cobalt(III) corrole where the anisotropy arises as a result of the low symmetry of the corrole ring (C_{2V}), or to a Co(IV) derivative. The observed rhombic signal with $g_1 = \sim 2.14$, $g_2 = 2.002$, and $g_3 = \sim 1.89$ suggests the formation of a low-spin d^5 Co(IV) complex with electron configuration $(d_{xz}d_{yz})^3d_{xy}^2$ or $(d_{xz}d_{yz})^4d_{xy}^1$ of the type discussed in the literature for related low-spin d^5 Fe(III) porphyrins.[41] The unresolved ^{59}Co hyperfine splitting may be indicative of some delocalization of the unpaired electron throughout the macrocycle. A splitting of the central line at $g = 2.002$ is also observed, and this is interpreted as resulting from an interaction of the unpaired electron with the ^{31}P nucleus ($I = {}^1/_2$) of the coordinated PPh_3 ligand. The coupling constant for this splitting is ~10 G.

A comparison of this coupling constant with the reported phosphorus–cobalt coupling constant of (TPP)Co^{II}(PPh$_3$) ($A_2 \sim 250$ G),[41] a species in which the unpaired electron is localized on the d_{z^2} metal orbital, may suggest some delocalization of the unpaired electron on the corrole π-ring system or simply reflect the fact that none of the orbitals which might be occupied by the unpaired electron (d_{xy}, d_{yz}, or d_{xz}) have a good overlap with the phosphorus atom of the PPh_3 ligand. Thus, one must conclude that the first oxidation of (OMTXPC)Co(PPh$_3$) is metal-centered resulting in formation of a low-spin d^5 Co(IV) species.

The fact that Co(III) corroles can undergo four one-electron oxidations was not previously reported, but presumably this reaction might also occur for (OMC)Co(PPh$_3$) at very positive potentials, *i.e.*, at values of $E_{1/2}$ greater than 1.9 V vs SCE in PhCN. The fourth oxidation of (OMTXPC)Co(PPh$_3$) is quasireversible for all eight compounds investigated in the present study, and this reaction was not examined in detail due to its proximity to the anodic potential limit of the solvent. However, a comparison of cyclic voltammograms for (OMT*p*-ClPC)Co(PPh$_3$) and (T*p*-ClPP)Co(PPh$_3$) (Figure 5) seems to rule out the fourth oxidation as involving the bound phosphine ligand.

Further comparison of the (OMT*p*-ClPC)Co(PPh$_3$) and (T*p*-ClPP)Co(PPh$_3$) voltammograms (Figure 5) shows that the first one-electron oxidation of both metallomacrocycles occurs at virtually the same potential, *i.e.*, + 0.31 V for the corrole and + 0.30 V for the porphyrin. The first oxidation of the neutral porphyrin corresponds to the Co(II)/Co(III) electrode reaction, while that of the corrole is assigned to the Co(III)/Co(IV) reaction.

The first ring-centered oxidation of the eight investigated corroles (process IV in Figure 5a) occurs at $E_{1/2} = 0.86-0.89$ V, values which are shifted negatively by ~400 mV as compared to the first ring-centered oxidation of related cobalt tetraphenylporphyrins (see Figure 5 and Table 3). In addition, the potential differences between the first and second ring-centered oxidations of the eight corroles (processes IV and V in Figure 5a) are also much larger (~0.65 V) than between the two ring-centered oxidations of the related Co(III) tetraphenylporphyrins (~0.21 V).[25] These results all suggest that the electron density distribution on the corrole cations differs substantially from that of the related Co(III) porphyrin cations. The more facile first ring oxidation of the corroles with respect to the first ring-centered oxidation of the porphyrins might also be due to the fact that the corrole is a tribasic ligand as compared to the porphyrin which is a dibasic ligand. The higher negative charge of the corrole trianion will thus increase the energy of the HOMO and lead to a much easier oxidation of the corrole macrocycle. This is in agreement with calculated energy levels of the corrole macrocycle where the energy of the HOMO is significantly higher than that of the porphyrin ring HOMO,[20] thus leading to a more facile removal of electrons from the conjugated π-ring system of the corrole.

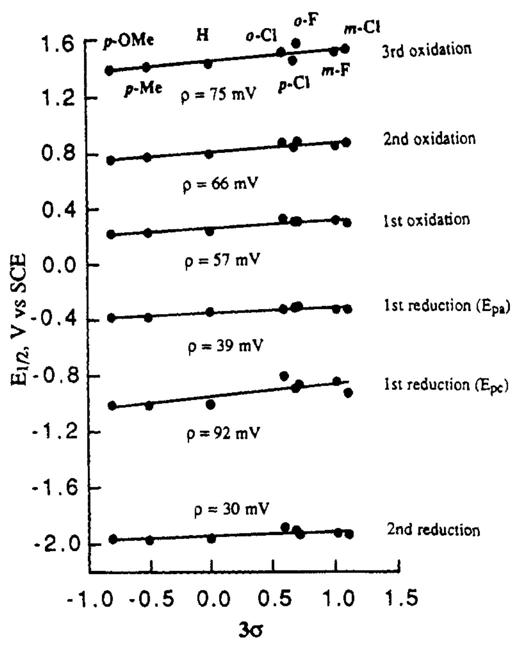

Figure 9. Effect of substituents on the redox potentials of (OMTXPC)Co(PPh$_3$) in PhCN, 0.2 M TBAP.

Substituent Effects. It has long been known that the addition of electron-donating or electron-withdrawing groups to the periphery of a porphyrin macrocycle will modify both the physical properties and the chemical reactivity of the compound. The effect of substituents on a given set of closely-related compounds can generally be quantitated by employing Hammett free energy relationships, which, for the case of redox potentials, is given by the following equation:[47]

$$\Delta E_{1/2} = E_{1/2}(\mathrm{X}) - E_{1/2}(\mathrm{H}) = \sum \sigma \varrho \qquad (3)$$

where σ is the Hammett substituent constant and ϱ, measured in volts, represents the sensitivity of the given redox reaction to the change of substituent. $E_{1/2}$(X) is the half-wave potential for the compound with substituent X, and $E_{1/2}$(H) is the potential for the compound with hydrogen as a substituent. The effects of substituents should be additive (if more than one substituent is present), and the change in $E_{1/2}$ for the investigated corroles which have three substituents can be defined as shown in eq 4.

$$\Delta E_{1/2} = 3\sigma\varrho \qquad (4)$$

Figure 9 illustrates how redox potentials of (OMTXPC)Co(PPh$_3$) vary as a function of the phenyl ring substituents. The first three reversible oxidations show a linear correlation between

---

(46) Wertz, J. E.; Bolton, J. R. *Electron Spin Resonance. Elementary Theory and Practical Applications*; Chapman and Hall: New York, 1986.

(47) *Advances in Linear Free Energy Relationships*; Chapman, N. B., Shorter, J., Ed.; Plenum Press: London, New York, 1972.

$E_{1/2}$ and the substituent constants (3σ). The values of ϱ calculated from the straight line plots using eq 4 are 57, 66, and 75 mV for the 1st, 2nd, and 3rd oxidation, respectively. These values can be compared with values of ϱ obtained for the two ring-centered oxidations of (TPP)Co which are equal to 100 and 130 mV, respectively, in PhCN.[29] The experimental values of ϱ obtained for the three oxidations are close to each other and cannot be used to distinguish between a substantially metal-centered Co(III)/Co(IV) process for the first oxidation and the supposedly ring-centered second and third oxidations.

The cathodic peak potential for the first reduction of the eight investigated corroles also follows a linear free-energy relationship and the plot of $\Delta E_{1/2}$ vs 3σ gives a slope of 92 mV. This value is rather high for a metal-centered Co(III)/Co(II) process and can probably be explained by the presence of the PPh_3 ligand and its subsequent dissociation, *i.e.*, the chemical reaction which follows the electron transfer. The ϱ value of 92 mV for reduction of the (OMTXPC)Co(PPh_3) complexes can be compared with a 39 mV slope obtained for the reoxidation process, a value more typical of a metal-centered Co(II)/Co(III) reactions, such as in case of (TPP)Co oxidation where $\varrho = 44$ mV.[29] The value of ϱ for the second reduction of (OMTXPC)Co(PPh_3) is 30 mV, which is about half the average ϱ found for oxidations of the same compound (66 mV). The Co(II)/Co(I) reaction of (TPP)Co also has a $\varrho = 44$ mV,[29] and this suggests a metal-centered Co(II)/Co(I) process during the second one-electron reduction of (OMTXPC)Co. It should also be noted that the potentials for oxidation or reduction of the two corroles having *o*-Cl or *o*-F substituents do not deviate substantially from the linear plots in Figure 9, thus indicating that *ortho*-substitution does not cause substantial ring deformation as is seen for the highly substituted porphyrins.[48]

Acknowledgment. Thanks are given to the MURST and CNR at the Università di Roma, Tor Vergata, and the Energy Laboratory at the University of Houston for financial support of this research. One of the authors (V.A.A.) is also thankful to the Electrochemical Society for an Energy Research Summer Fellowship Award. We also acknowledge the helpful comments of Dr. F. Ann Walker with respect to analyzing the EPR data of the electrooxidized compounds.

IC9408765

---

(48) (a) Barkigia, K. M.; Chantranupong, L.; Smith, K. M.; Fajer, J. *J. Am. Chem. Soc.* **1988**, *110*, 7566–7567. (b) Barkigia, K. M.; Renner, M. N.; Furenlid, L. R.; Medford, C. J.; Smith, K. M.; Fajer, J. *J. Am. Chem. Soc.* 1993, *115*, 3627–3635.